Thesis Title

A subtitle of your thesis

Author name

Thesis submitted for the degree of
Master in Master's Program Name <change at
main.tex>
60 credits

Department Name <change at main.tex>
Faculty name <change in duoforside.tex>

UNIVERSITY OF OSLO

Spring 2022

Thesis Title

A subtitle of your thesis

Author name

Abstract

Contents

List of Figures

List of Tables

Preface

Chapter 1

Introduction

some introduction on the importance of discovering new materials and alloying.

High-entropy alloys is a novel class of materials based on alloying multiple components, as opposed to the more traditional binary alloys. This results in an unprecedented opportunity for discovery of new materials with a superior degree of tuning for specific properties and applications. Recent research on high-entropy alloys have resulted in materials with exceedingly strong mechanical properties such as strength, corrosion and temperature resistance, etc **find references**. Meanwhile, the functional properties of high-entropy alloys is vastly unexplored. In this study, we attempt to broaden the knowledge of this field, the precise formulation of this thesis would be an exploration on the possibilities of semiconducting high-entropy alloys.

A key motivation of this thesis is the ability to perform such a broad study of complex materials in light of the advances in material informatics and computational methods. In this project, we will employ Ab initio methods backed by density functional theory on top-of the line supercomputers and software. 20 years ago, at the breaking point of these methods, this study would have been significantly narrower and less detailed firstly, but secondly would have totaled ... amount of CPU hours to complete (**Calculate this number**). In the addition to the development in computational power, is also the progress of modeling materials, specifically we will apply a method called Special Quasi-random Structures (SQS) to model high-entropy alloys or generally computationally complex structures. Together with the open landscape of high-entropy alloys described above, these factors produce a relevant study in the direction of applying modern computational methods to progress the research of a novel material class and point to promising directions for future research.

In specifics, this thesis revolve around the electrical properties of high-entropy alloys, mainly the band gap as this is the key indicator for a semiconducting material and it's applicability. Semiconductors are the building blocks in many different applications in today's world, ranging from optical and electrical devices, to renewable energy sources such as

solar and thermoelectricity. Given the economic and sustainable factors concerning silicon, in addition to its role in relevant applications such as microelectronics and solar power. Silicon emerges as a natural selection to build our alloys around. Furthermore, the development and research on both high entropy alloys and metal silcides have been heavily centered around 3d transition metals. Keeping in line with the economic and environmental factors, we will continue this direction by focusing on high entropy stabilized sustainable and economic 3d metal silicides **Not happy with this writing**. Throughout the study we will analyze a great number of permutations of 3d silicides, from different initial metal silicides such as $CrSi_2$, $FeSi_2$, $MnSi_{1.75}$, Fe_2Si, each with distinct properties relating to the band gap, crystal structure and metal to silicon ratio. In addition, the permutations include numerous metal distributions and elements within the 3d-group of metals. Examples are Co, Cr, Fe, Mn, and Ni.

Given a background in high-entropy alloys, one could ask if this study is truly sensible. In the later sections we will cover the details of this field, and it quickly become clear that the materials investigated in this study does not fall under the precise definition of high-entropy alloys, nor do we intend to explore the properties and factors relating to high-entropy stabilized alloys such as the configurational entropy, phase stability and finite temperature studies. However this study is motivated from the discovery of these materials and promising properties, and venture into a more hypothetical space of materials, enabled by the computational methods available to study the potential properties of such materials. On the other hand, very recent studies **Mari, and other HEA silicide study** have experimentally produced high-entropy disilicides, thus in some way justifying the direction of this project.

We begin this project by reviewing key concepts of solid-state physics for readers lacking a background in materials science, and an introduction to the base 3d silicides of the experimental work. Later follows a theoretic walk-through of the relevant concepts of this thesis, these topics include high-entropy alloys, special quasi-random structures, and density functional theory. Next we shine light on the implementation of DFT in this project, and other computational details required to reproduce the results in this thesis, such as the use of the Vienna Ab Initio Simulation Package (VASP) and implementation of SQS. Finally we present the results of our study, these include the band gap and electronic properties of various structures and the success and challenges of the computational methods applied throughout the study.

Part I

Theory

Part II

Methodology and Implementation

Part III

Results and Discussion

Chapter 8

The good (CFMN fesi2)

In this nearly two year long study, we have managed to investigate a great number of materials with various structures and compositions. We initially began by experimenting with an Fe_2Si unit cell and create these high-entropy silicides by using the special quasi-random structure approach as described above. All though this initial compound is not a semiconductor, we worked under the hope that the extraordinary properties that have been observed in high-entropy alloys through effects such as the cocktail effect, we could locate a specific combinations of elements that in terms would yield a semiconductor with unchanged metal to silicon ratio. Thus creating a highly efficient thermoelectric material based on the other suitable properties of di-iron silicide. All though this idea is not invalidated, because there are plenty-full of else compositions and permutations to trial, in our narrow search we however did not find such a material. Therefore we opted for a more conservative angle for our study by instead considering well known semiconducting TM silicides such as $\beta - Fe_2Si$, $CrSi_2$ and $MnSi_{1.75}$, see section .. for an introduction to these. However, also for these disilicides we experiences limited success in finding semiconducting materials. In fact, the only case in which we found positive confirmation of a band gap was for a particular composition of $(Cr_{0.25}Fe0.25Mn_{0.25}Ni_{0.25})Si_2$, here-in CFMN, in the $\beta FeSi_2$ configuration. This make for an interesting question that we will try to understand and answer in this section, why is exclusively this compound semiconducting?

We will try to answer this question by first considering the CFMN (fesi2) compound, and investigating the potential properties and correlations between the different elements that make this particular system semiconducting. Factors we will investigate is the overall stability by total energy per atom and formation enthalpy, the magnetic configuration and which elements contribute the magnetism. But in majority, we will look at the band gap and related properties, as this is the main motivation and distinction of the study. When we are done analyzing this system, we will transition into the similar compounds we have worked with in this project, but that turn out metallic. First we will look at compounds within the same crystal structure, but where we substitute the exact composition of $(Cr_{0.25}Fe0.25Mn_{0.25}Ni_{0.25})Si_2$ with other 3d elements and distributions

slightly away from eqvimolar. Then we present the results of the CFMN composition in different crystal structures mentioned above, ie Fe_2Si where we flip the metal-silicon atom ratio, $CrSi_2$ where the ratio is consistent, but in a different crystal structure, and $MnSi_{1.75}$ where we alter both simultaneously. Finally we will compare and discuss the observed distinctions and give our thoughts on the complete experiment and guideline future research directions in this field.

8.1 Eqvimolar distribution

In section .. we briefly discussed various semiconducting TM silicides, such as $\beta - FeSi_2$ in the orthorombic cmce lattice. In our DFT work, we find this structure semiconducting with an indirect band gap close to 0.65 eV with PBE. Additionally we found the compound to be non-magnetic and a total energy per atom equal to 6,8274 eV. Which means that we can calculate the formation enthalpy as $\Delta H = E/at_{FeSi_2} - (E/at_{Fe} + E/at_{Si}) = 7{,}0653$ eV, with the help of materials project for providing the total energy per atom for iron (-8.4693 eV) and silicon (-5.4234 eV).

The $FeSi_2$ structure consisted of 48 atoms, 16 of which is iron and the remaining 32 sites occupied by silicon atoms. In our project, we filled the 16 iron sites with an even distribution of chromium, iron, manganese and nickel by the principle of the SQS method described in section .. . With this approach, there are many possible supercells one can create, we however limit our-self to 5 distinct supercells per composition, which means that we have 5 structures of the same composition and space group, but the distribution is slightly different. This allow us to both study a composition to great depth, but also to test different compositions and structures, compared to if we instead generated 10 or 15 or more supercells. But its important to be aware of this assumption, as our results may be subject to errors and result that does not match the true random alloy due to a small sample size.

Bellow in table .. we display the most relevant properties to the 5 SQSs of the CFMN (fesi2) system for this study, they are the total energy per atom, final magnetic moment per atom, and the band gap. For simplicity, we denote these SQSs as A, B, C, D and E.

Structure	Total energy/atom (eV)	Final magnetic moment/atom (?)	Band gap (eV)
A	-6,6080	0.0833	0.0280
B	-6,6138	0.0833	0.0523
C	-6,6063	0.0834	0.0344
D	-6,6155	0.0833	0
E	-6,6089	0.0833	0.0495
Mean	-6.6105	4.0000	0.0328
Std	0.0039	0.0000	0.0210
ΔH_{mean}	-11.5000 eV	-	-

Table 8.1: Total energy per atom, final magnetic moment, band gap (GGA) and formation enthalpy of $Cr_4Fe_4Mn_4Ni_4Si_{32}$ SQSs based on $FeSi_2$

From a first glance, we observe very similar properties between the structures regarding both the total energy and final magnetic moment. **Something on stability**. Comparing to $FeSi_2$, by replacing purely iron atoms with a number of 3d elements we have made the compound magnetic. We performed self-consistent total energy calculations with ispin=1, ispin=2 and ispin=2, MGMOM=2*NIONS **What does this mean?**, and found that ispin2 was the most stable magnetic configuration. The consistent magnetic moment between the 5 supercells is excpected seeing as all 5 structures consist of equivalent elements. The magnetism is as attributed solely from 3d electrons and in particular from chromium and manganese, whereas the iron and nickel atoms are diamagnetic. **Near 0, or negative values in OUTCAR**.

The most interesting property of these SQSs is in fact the band gap. We note a mean band gap of about 0.03 eV, in contrast to 0.65 eV in bulk $FeSi_2$. The gap is seen in 4 out of 5 SQSs, but surprisingly not in the most stable arrangement (D), the largest gap observed is about 0.05 eV from structure B, which is very similar to D in terms of total energy. Moreover the gaps are indirect, the transitions is listed bellow in table .. .

Structure	Gap (D/I)	Transition
A	I	(0.500,0.333,0.500)-(0.500,0.000,0.000)
B	I	(0.250,0.000,0.250)-(0.000,0.000,0.000)
C	-	(0.500,0.000,0.500)-(-0.250,0.333,0.500)
D	I	-
E	I	(0.000,0.000,0.000)-(0.250,0.000,0.250)

Table 8.2: Band gap transition of CFMN (fesi2) SQSs with PBE functional

A very useful method to extract information regarding the band gap of a material is to plot and study the band structure, however this is not as insightful when considering large supercells with large number of energy bands. The solution to this is normally to do a band unfolding, but given the complex structure and implementation of these SQS is VASP we

where not able to do band-unfolding or plot the band structure in any way. Another method to study the band gap is to observe the density of states, in figure .. we plot the total density of states. In these plots, the 0 value on the x-axis is set to the Fermi energy, in other word the negative values relate to states in the conduction band and positive values the valence band.
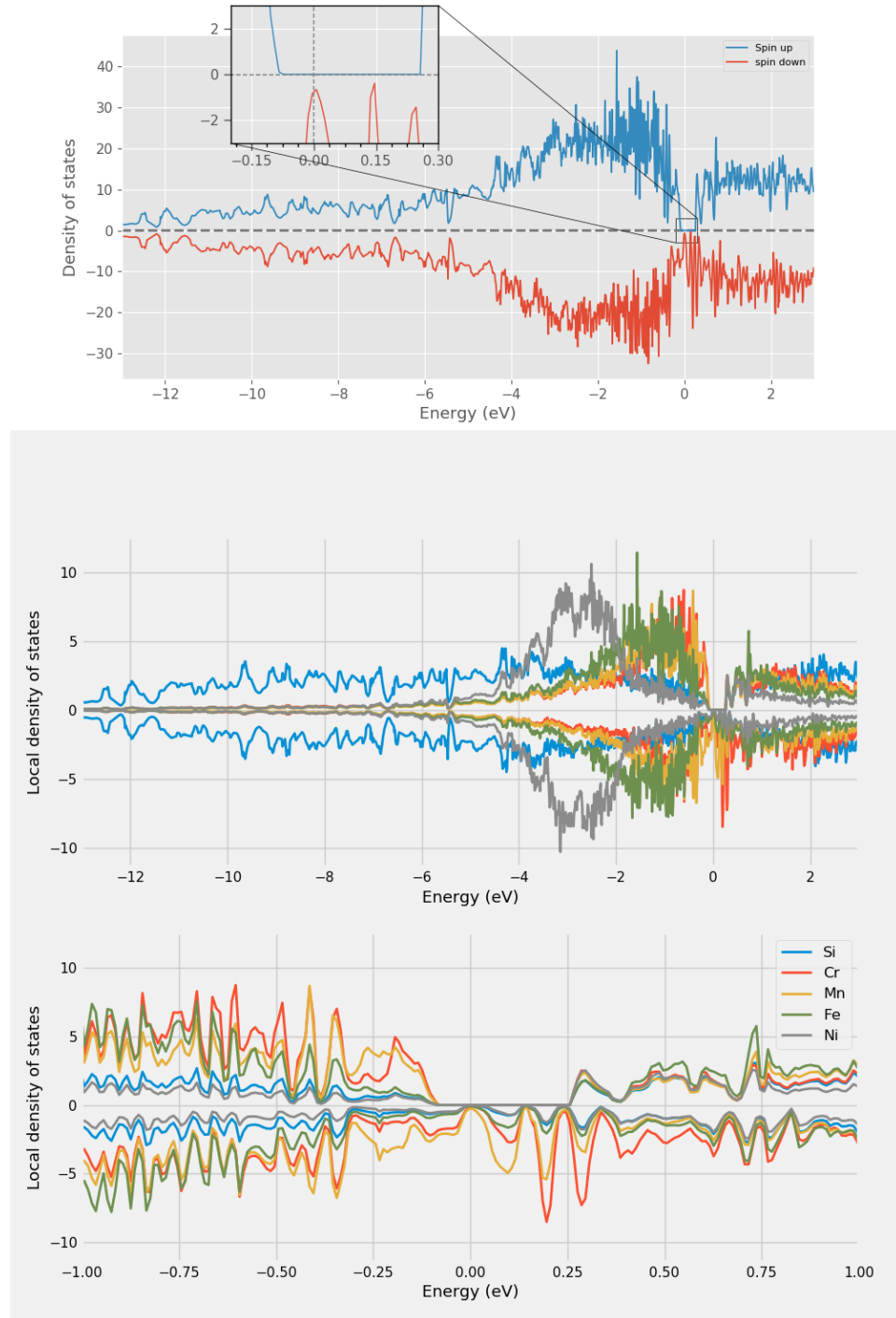
In spin polarized materials such as this one, the band gap can be

extracted from the total DOS by the minimal width of unoccupied states around the Fermi energy. From figure .. we can observe two properties of the band gap. One, there is clearly a band gap in structures A, B, C, and E, and secondly, the band gap is significantly greater in the spin $\uparrow$ channel than spin $\downarrow$. This is especially evident for structure D, where we learn that the structure is metallic in spin down, but contain a sizable gap in spin up.

The density of states, all though useful provide limited information. For instance, the DOS in structure D point to a difference in spin states, but does not give any indication as to to why. Additionally, the density of states can be unreliable and prone to errors. As mentioned in section .., the smearing is important for accurate DOS calculations, preferably the tetrahedron smearing with Bloch correlations (TBS). In this project we experiences a significant difference between calculations with gaussian and TBS smearing in relation to the written band gap and the density of states band gap (More on this later). Moreover the DOS is very sensitive to computational factors such as number of points used in the DOS (NEDOS in VASP) and k-points (to solve the DOS integral, see section ..). For example, the band gap in structure C could only be seen in the density of states when increasing the number of points in the DOS from 2401 to 20000 points (this was not the case for the other structures).

Structure	Spin-up	Spin-down	Total
A	0.0814	0.0522	0.0281
B	0.2932	0.0523	0.0523
C	0.2355	0.0343	0.0343
D	0.3386	0	0
E	0.3078	0.0495	0.0495

Table 8.3: Band gap (eV) with PBE in spin up and spin down channels of CFMN (fesi2) SQSs

A more rigid method for both determining and investigating the energy bands is to study the Kohn-Sham eigenvalues. The eigenvalues are given for all energy bands for the given number of k-points used in the calculation, with listed energies and corresponding occupancy in both channels. In table (..) above, we provide the relationship between the spin up and down channels in regards to the band gap, as read from the eigenvalues. In addition to validate and quantify the point expressed above about the gap in both spin channels, we can from the eigenvalues qualitatively differentiate structure D from the rest. From observing that for certain k-points, the occupancy does not transition from 1 to 0 directly between two bands, but rather contain one or more partially occupied bands in between, however only in the spin down channel. If we were to neglect this partially occupied states, and only consider bands with above 0.99 or bellow 0.01 occupancy, the band gap of structure D remain consistent in spin up, but we now observe a band gap in spin down around 0.05 eV and similarly thus for the total band gap of the structure. Again,

this would have been extremely insightful to investigate with help of a band structure diagram.

Something on the flaws of EIGENVALUES, bloch corrections yield un-physical eigenvalues in structures without band gap. Some times we find band gap from eigenvalues but not DOS or other script. What does the distance in bands between 1 occ and 0 occ mean?

As expressed previously, in this work we include 3 level of depths GGA (PBE), meta-GGA (SCAN) and hybrid functionals (HSE06). In table .. bellow we show the results from these functionals.

Structure	PBE	SCAN	HSE06
A	0.0281	0.0000	0.0207
B	0.0523	0.0890	0.1808
C	0.0344	0.0690	0.0196
D	0.0000	0.0000	0.0000
E	0.0495	0.1048	0.0133

Table 8.4: Band gap of $CFMN(FeSi_2)$ SQSs with GGA (PBE), meta-GGA (SCAN) and hybrid-functionals (HSE06).

The first fact we make notice of is that aside from A, all 3 methods agree on the presence of a band gap, but the actual value is under debate. We see a general trend that the SCAN functional find the largest gaps and HSE06 the lowest. This is an unexpected result, the general consensus is that hybrid functionals will extend on the band gap found by LDA or GGA functionals **Find reference!**. However we find one exception to this trend, in structure B the band gap increase from 0.05 to 0.09 and 0.18 eV. The most likely reason for this abnormal large gap is a consequence of the small number of k-points we had to employ in order for the calculations to converge. Recalling that the transition in in the PBE calculation was (0.250,0.000,0.250)-(0.000,0.000,0.000), comparing to HSE, the gap transition is between (0.500,0.000,0.000)-(0.000,0.000,0.000). Moreover, the point (0.250, 0.000, 0.250) in k-space is not included in the hybrid functional due to the narrow mesh (from IBZKIT file). Thus we may conclude that the large gap from HSE06 is a result of that the minimal gap is not encapsulated by the k-mesh. On the other hand, with the SCAN functional we also observe an increased band gap, and also a different band transition from (0.250,0.000,0.250)-(0.000,0.333,0.000) despite identical k-points used in PBE and SCAN. We find the same results in the other SQSs as well, ie that the band transition varies between the 3 functionals of the same SQSs.

The most relevant result regarding the SCAN functional is that of structure A, in which both PBE and HSE06 finds a semiconductor, but SCAN does not. Similar to structure D, this is because the eigenvalues contain so-called defect states and non-physical occupancy. Neglecting these, we find a band gap of about 0.03 eV, which is in good agreement with the PBE value.

With the HSE06 functional we find a band gap of 0.021 eV, with a transition (0.000, 0.500, 0.500) - (0.500, 0.000, 0.000). From the eigenvalues we find that the gap is 0.7 eV in the spin up channel, compared to 0.02 eV in spin down and total **See DOSCAR maybe?**. As stated previously, to converge HSE06 calculations we had to first perform the calculation with Gaussian smearing, then reapply the charge density of that calculation to perform the calculation again with TBC smearing. Interestingly, the result of the first calculation (Gaussian) yielded a band gap of 0.15 eV, (0.78 up and 0.15 down). However the eigenvalues contain defect states and is not apparent from the density of states. Without defect states the band gap is increased further to 0.25 eV. By reducing the smearing width from 0.05 to 0.005 we find a gap of 0.1 eV (0.21 up and 0.1 down) without any defect states, and that is shown in the density of states. **Include figure?**

In structure B, we have calculated the band gap with both gaussian and TBC smearing for PBE and HSE06. From PBE, both methods agree on a band gap around 0.05 eV, but the gaussian method yield eigenvalues with defect states, and a metallic density of states. Without defect states the band gap from gaussian PBE is found to 0.17 eV. In this supercell, the SCAN functional find a total band gap of 0.088 eV from 0.15 eV up and 0.088 eV down, the eigenvalues are pure and the gap is well represented in the density of states. The hybrid functional of this SQS is in pretty good agreement despite of smearing method. From gaussian smearing and smearing width we find a gap of 0.15 eV (with defect states, 0.28 eV without). From reducing the smearing width we find a gap of 0.18 eV identical to TBC, without defects in the eigenvalues and represented in the density of states.

Structure C is similar to B with PBE, where the smearing method produce similar band gaps, but the gaussian contain defect states. Interesting of this structure is that the SCAN functional result in an opposite gap to the PBE functional. With PBE, the gap was largest in spin up and limited by the down states. From Scan, we observe that the gap is about 0.11 eV in down, and 0.07 eV in up. HSE06 agree with PBE, and find that the spin up channel have a band gap of 0.17 eV and 0.032 eV in spin down. With gaussian smearing, we find HSE06 to yield a gap around 0.1 eV in both channels and 0.065 eV in total (with defect states).

In structure D, we observe the same result. From PBE, the we find a band gap in spin up around 0.33 eV, but a metal in spin down. If we remove the defect states, the spin up gap remain constant, but we now find small gap of around 0.05 eV in down and correspondingly in total. And from the SCAN functional, the inverse is true. ie we initially find a band gap for spin down electrons, but not spin up. The results of HSE06 for this supercell is similar to structure C, in agreement with PBE and disagreement with SCAN. The band gap from HSE06 is calculated to about 0.37 eV in up and 0 in down from gasuusan smearing. We find a total gap of 0.26 eV when overlooking the defect states in the eigenvalues. **Wait for ismear-5 HSE06 to finish**.

Finally, we observe the same pattern again for structure E. The PBE functional find a large gap in up and near 0 in down with TBC smearing.

And the gaussian smearing find a similar gap in spin up, and the small gap in spin down is consistent, but caused by defects. Removing these defects we find a gap in down around 0.16 ev resulting in an increased total gap. Also in this case, the SCAN functional finds a different band transition than PBE, despite identical k points and parameters. The gap is calculated to 0.15 eV in spin up, 0.11 eV in down and 0.10 in eV in total. The HSE06 calculations of this structure resemble that of structure A. With TBC, the band gap is very large in spin up, about 0.55 eV, but close to 0 in down. The gaussian smearing finds similarly a large gap in up (0.66 eV) and a larger spin down gap around 0.15 eV, with defect states and 0.16 eV without. This gap is not apparent in the density of states, but we have found merit that the gap could become viable, by reducing the smearing width, as in structure A.

A concluding remark, why does only str B agree between gaussian and TBC in HSE06. And which method is more reliable, surely one would expect the gaps from HSE06 to be bigger than PBE/SCAN. But the tetrhaedon method is considered the most accurate? **This is discussion material!, rewrite this section, and try to make the summary more concise and less repeative, while still containing the same information**

At the risk of becoming repetitive and tedious, we still include this section where we walk though every SQS and the 3 functionals to make the reader aware of the differences and and disagreement we have observed in this study, both in relation to 5 SQSs of the same compound, but also from three highly praised exchange-correlation functionals. In conclusion, its very strange that the two smearing methods produce the same band gap in several instances, but that one of the channels is caused by defects in gaussian, but TBC find the same gap but without defects. And in addition, the large differences observed for HSE06 between the two methods is interesting. **I think I will include something like this in the summary/conclusion: Due to the disagreement between methods, SQS'sizes and etc, we may not confidently report a precise value of the band gap, but we can with some confidence conclude that we have found semiconducting high-entropy silicides.**
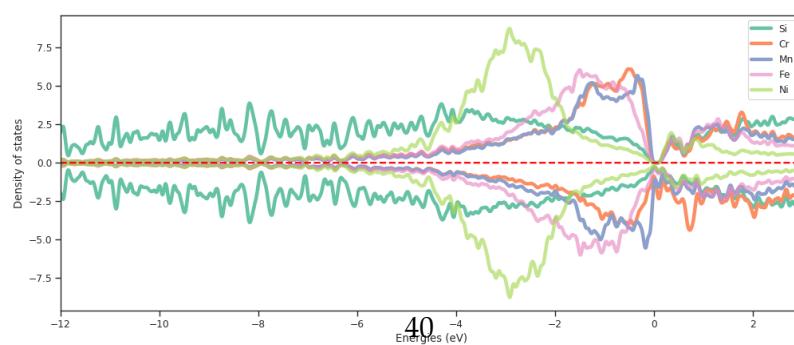
To further compare and anlyze the 5 SQSs of CFMN (fesi2) high-entropy silicide, we investigate the local density of states (LDOS), given in figure **insert ref. These figures needs work for how they are presented, include all? Or just 1?, full view or zoomed around EF, fix axes ticks font size and weight and figure size. Redo structre C with the DOS from NEDOS**
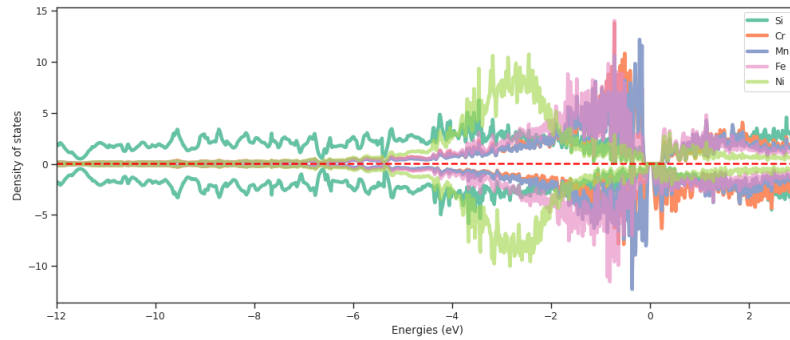
(a) A

(b) B

40
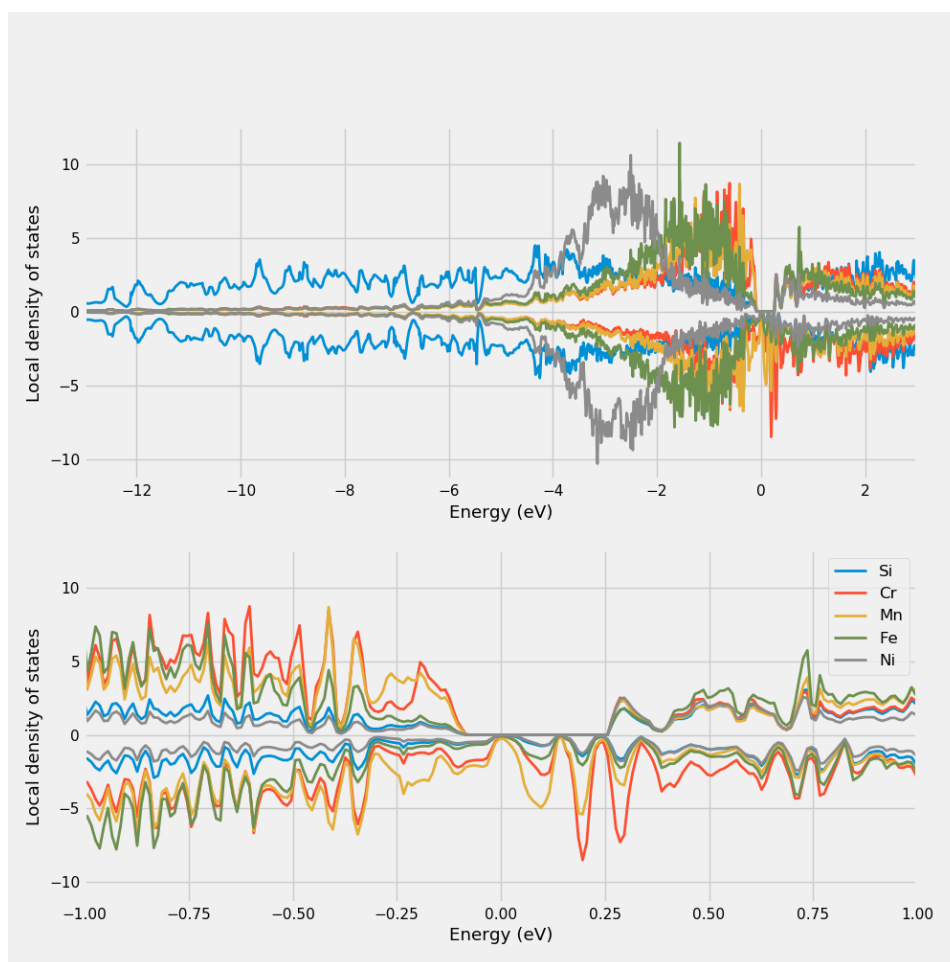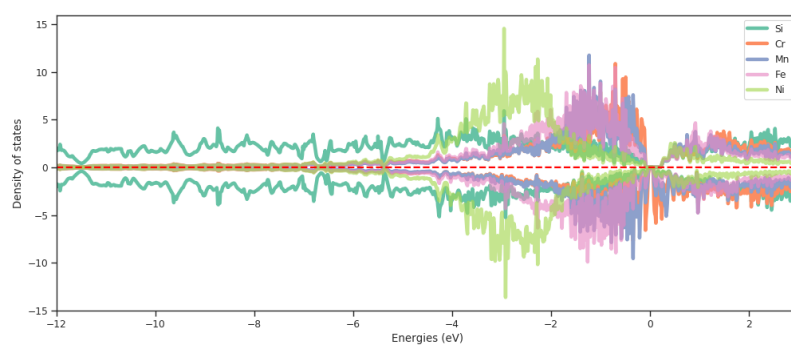
(c) C

Figure 8.3: E

From these figures, we observe a typical pattern throughout the 5 SQSs, in which energies much lower than E_F is dominated by s electrons corresponding to silicon atoms. At slightly higher energies, we see strong hybridization of Si p electrons and 3d electrons of TMs. We observe for both spin channels that Ni lie at the lowest energies of the 3d elements, followed by iron and then manganese and chromium very close to the fermi energi. Above the fermi enery, we obsere a more equal contribution from all elements, however energies slgihtly above EF is slightly favored by Fe in spin up states, and Cr in spin down. For higher energies, the highest LDOS is attributed to Si and Cr, while elements such as Ni, Fe and Mn have a lesser role on the total DOS. One key distinction of str D is a heavy amount of Manganese at energies right above Ef in spin down, in contrast to the other structures that are dominated by Cr at this energy. An additional distinction between the five SQSs is the intensity of the local density of states, in the structures with the highest band gap, structures B and E, the local density of states is slightly higher. In particular, structure E show high LDOS of Cr and Mn close to Ef in spin up, and Ni in structure B at slightly lower energies.

If we now consider the probability distribution functions (PDFs), shown in figure **insert ref!**. From these figures there is a lot of useful information to investigate. With the aid of the ICSD (insert citation), we can locate the expected PDFs based on recent research and experiments from a host of different compounds. As our compound contain a total of 15 different bonds, comparing each one of these for all 5 supercells to the ICSD values would be an exhaustive process. For our purpose we are satisfied by comparing the 4 different metal-Si bonds and note ourselves of key distinctions. We find that the preferred bond-length of TM-Si is observed at two values, the most dominant being the shorter of the 2. For Fe-Si these are between 2.25-2.75 and 4-5, Mn-Si 2.25-2.75 and 3.5-5. Ni-Si lie between 2.25-2.5 and 3.85-5 and Cr-Si between 2.35-2.65 and 4-5.
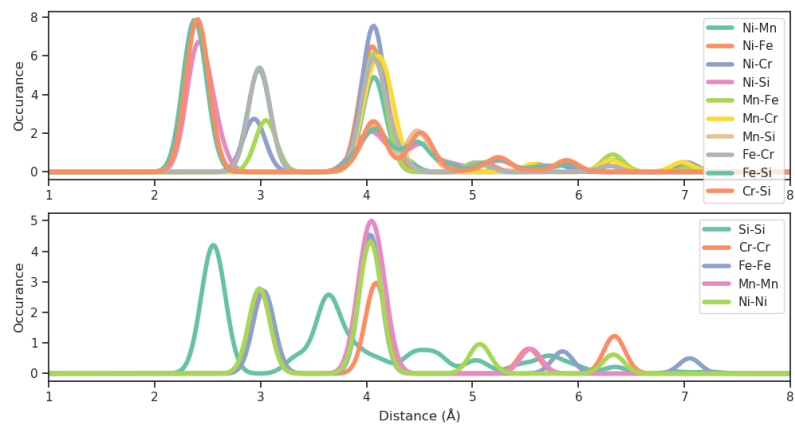
These figures need work, maybe not include all or? I notice that the same color is used twice several places, also some lines are covered by other. To actually read info from these I had to study them in matplotlib and zoom in and out

41

(a) A

(b) B

(c) C

42
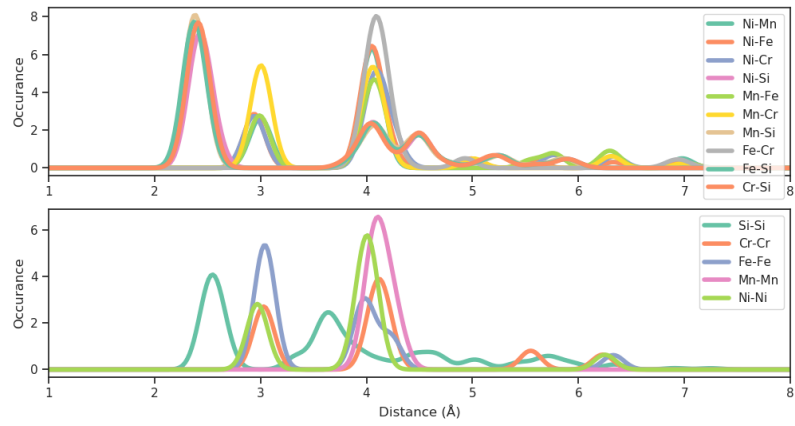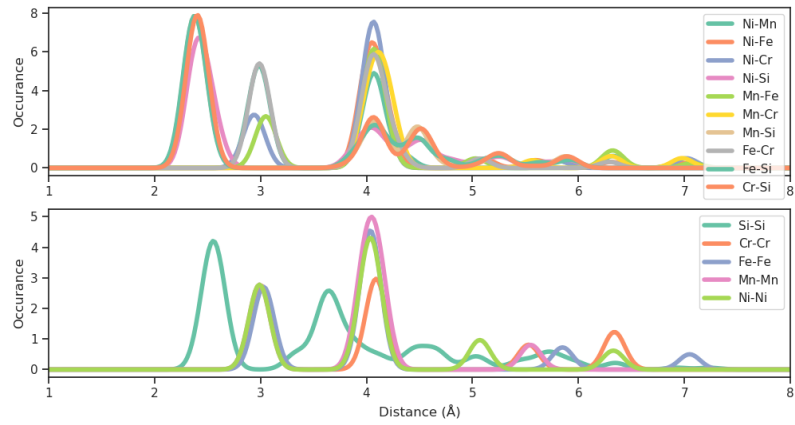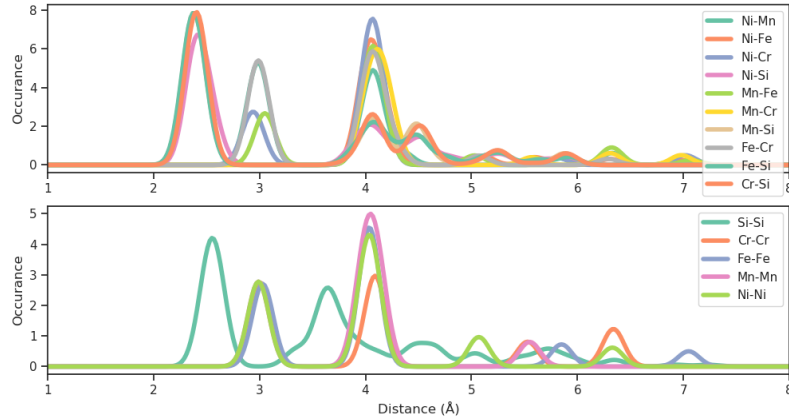
(a) D
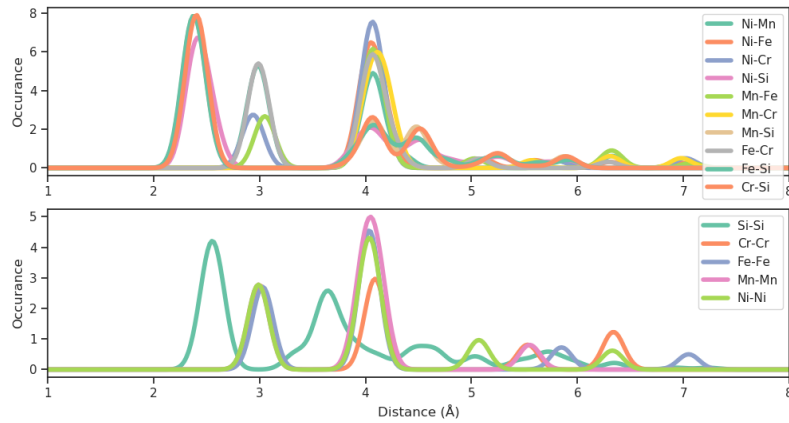
(b) E

Finish discussion pdfs, introduce CHGCAR

At the surface, figure .. show that are supercells are in good agreement with the listed values for Tm-Si bonds, with the most occurring bond length falling at around 2.4 Å for all TMs, and some bonds at around 4.1 Å. The relative height of the peaks follow a similar trend, Fe-Si, Mn-Si, and Cr-Si all lie close to 8 for the first peak at 2.4 Å, and Ni-Si slightly bellow around 7. **More on the PDFs?**

Lastly we include the charge density of blabla, **something on these.**

8.2 Permutations

Up until this point we have investigated the structure CFMN ($FeSi_2$). Morre specifically we have looked at the center of a quasiternary pahse diargram. In this section, we aim to exapand our search of this diargram by studying SQSs slightly away from eqvimolar distribution of 3d elements. In table (bellow) we list the mean total energy and magnetic moment per atom with corresponding standard deviation, and enthalpy of formation of 4 different
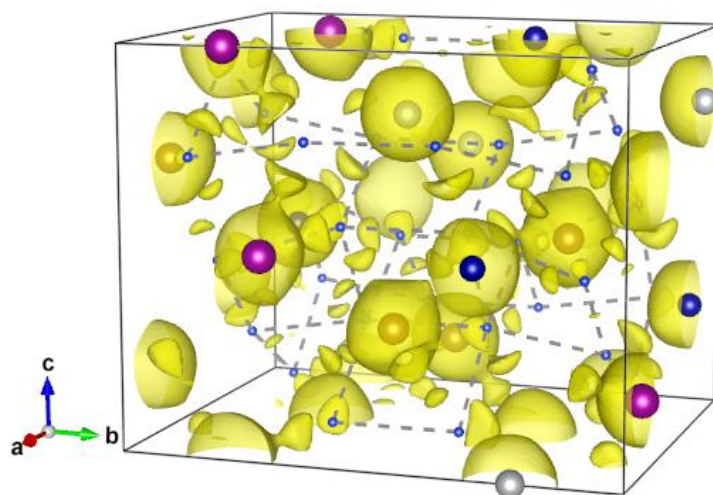
(a) Structure B
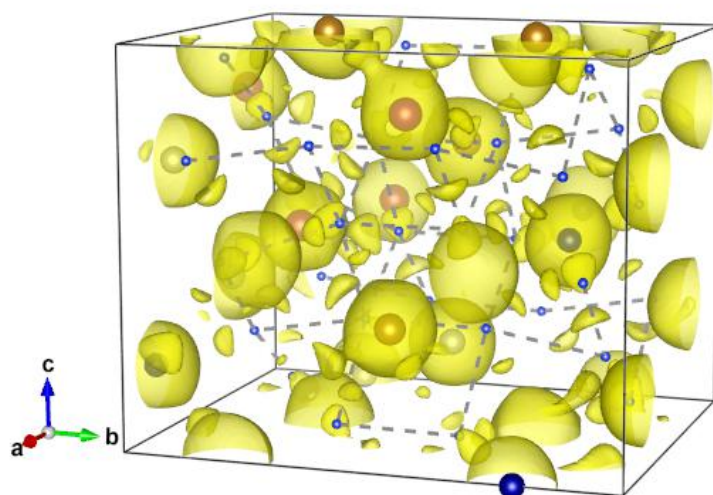
(b) Structure D

permutations of the quasiternary phase diagram. Ideally we would like to only alter one element at a time, but the TDEP method insist in also reducing Nickel to stay consistent with the 48 atom supercells. The 4 permuations are listed bellow

	Toten (eV)		Enthalpy of formation	Mag	
$Cr_3Fe_3Mn_7Ni_3Si_{32}$	6.6947	0.0040	-11.9586	0.1375	0.0186
$Cr_5Fe_5Mn_3Ni_3Si_{32}$	6.6705	0.0030	-11.1991	0.1127	0.0223
$Cr_5Fe_3Mn_5Ni_3Si_{32}$	6.6852	0.0041	-10.5200	0.1375	0.0456
$Cr_3Fe_5Mn_5Ni_3Si_{32}$	6.6801	0.0036	-12.6426	0.0937	0.0209

Table 8.5: Mean and stadard deviation of the total energy and magnetic moment per atom, plus enthalpy of formation of the listed mean energies ($FeSi_2$).

Interestingly we find that we can increase the stability of the compound by adjusting the distribution of 3d elements. The most stable permutation is found when we increase the amount of manganese relative to the other TMs. In said permutation we find very similar properties as the equal distribution in terms of the band gap. From PBE calculations, we find that the band gap ranges from 0.13-0.47eV in spin up, depending on the supercell and all except for structure D have zero gaps in down, here we find a total band gap of 0.0063 eV. In contrast to equally distributed CFMN (fesi2), the SCAN functional does not find a band gap in any of the five supercells, except for small gaps less than 0.06 eV in spin up for structures D and E. Extending to the HSE06 functional, we find that structre D contain a large band gap of 0.17 eV, 0.57 eV and 0.26 eV in spin up and down respectfully. Both the gaussian and TBC smearing method are in excellent agreement of the gap. Howver, the result of the hybrid functional are surrounded by the same factors of uncertainty as described for CFMN (fesi2), in that also in this case we find that the transistion of the indirect band gap is sensetive to the applied functional and escpecially the limited number of k-points used to perfrom HSE06 calculations.

If we now move in the opposite direction and reduce the number of manganese atoms we observe the opposite, namely the least stable permutation in terms of the total energy. One of the 5 SQSs (D) is a semiconductor, this supercell show from PBE calculations a band gap of 0.067 eV (up) and 0.041 eV (down) and 0.037 eV in total. The SCAN functional in contrast predict a half-metal with a band gap of 0.17 eV in spin down. The conflicting band gap contunue with the HSE06 functional, resulting in 0.77 eV in spin up and 0.22 eV in down and total. Thus PBE and HSE06 result in a semiconductor with HSE06 pointing to a large spin polarization and PBE finding symetric spin values. And on the other side, meta-GGA calculations predict a half-metal with semiconduction in the spin-down channel, opposiste of the polarization from HSE06. As follows drawing a conclusion on the band gap is challanging, but as discussed previosly we emphazie the results of GGA and hybrid functionals for the

univeral application and reputation they hold in self-consistent method studies of electronic structure.

The two most stable SQSs C and E, both exhibit large band gaps soeley in the spin up channel. These gaps contain a few partially occupied bands that result in the gap vanishing in the density of states. This is an interesting result, as opposed to structures where many bands are partially filled, the structure is obviosuly a metal as apperant from both the calculated band gap and density of states. But in cases where there are only very few states with partial occupation we see a band gap from the eigenvalues and also the density of states show indication of a band gap with the DOS becomming very low near the fermi energy, but not exactly zero as in the structures with no partial occupants.**Include DOS figure??** The spin up band gap in C and E discussed above is calculated from the eigenvalues as 0.21 and 0.36 eV respectfully. In both cases the gap vanishes with SCAN, and HSE06 calculates unfortunatly proved difficult to converge for these structures, thus we were unable to obtain results with the hybrid functional. A positve conclusion of this permutation, is that if we include the possible half-metal gaps in C and E, we can report that the most stable arrangements are half-metals, then semiconducting and the least stable SQS is metalic. In conclusion we can then state that semiconducting and escpecially half-metalalic are the preffered state over metallic in this permutation.

$Cr_5Fe_3Mn_5Ni_3Si_{32}$ is on par with $Cr_5Fe_5Mn_7Ni_3$ in terms of both stability and magnetism. We note that the high magnetic moment is mostly attributed to the least stable SQSs, and the more stable arrangements have magnetic moment 5/48, as opposed to the first permutation in which we found high magnetism also in the stable SQSs. From PBE GGA calculations we obtain spin-polarized half-metals in structures A, B, C, and E with the spin up gap ranging between 0.21(A)-0.47(C) eV. Wheras structure D is a semiconductor with a 0.012 ev band gap (slightly larger in up than down). Additionaly this is also the most stable SQS second only to A. In most cases, the use of SCAN results in very small spin up gaps, the rest 0. From the hybrid functional we find very conflicting results of strcture D. With TBC smearing, HSE06 predict a metalic gap , but we see signs in the density of states that may indicate a half-metal in spin down **Figure?**. Using instead the gaussian smearing method results in a gap of 0.063 eV and 0.27 eV in spin down with some partial occupancy in both channels, but much rarer and less impactfull in the spin down states (Similar DOS as TBC).

Lastly, the final permutation we did of CFMN (fesi2) was to reduce the amount of Cr. The most dominant display of this is the magnetism, out of the 4 permutations and the baseline system, this was the least magnetic system, according to our calculations with a fixed magnetic configuration. This is not a surprising result recalling that in CFMN fesi2, the magnetic momemt was primarly attributed to Cr atoms in the lattice. We find 2 semiconductors (D and E) and 2 half-metals (A and C). Similar to the other systems discussed in this section, the half-metals display a sizable band gap in the spin up direction, 0.39 eV and 0.12 eV respectfully. SCAN calculations result in stucture A being a semiconductor with a band gap

of 0.015 eV, and B a metal. Of the two semiconductors, both PBE and SCAN agree of a band gap, PBE predict a band gap of 0.1 eV (0.25 up and 0.1 down) in D, and 0.014 eV (0.21 up and 0.08 down) with SCAN. In contrast to both, HSE06 calculations produce a semi-metal with a spin up gap of 0.53 eV. In E we find a band gap of 0.35 and 0.10 eV in the two spin directions, yielding a total gap of 0.084 eV. The SCAN calculations find several nonphysical eigenstates and thus no band gap. From HSE06, we find as before greatly exatereded band gaps of 0.74 eV in spin up, and 0.25 eV in total. An additiontal positive regarding this permutation is that the two semiconducting SQSs are the most stable of the set, with D having the highest total energy, followed by E. The least stable supercell is A, it's important to note however that the total energy very similar across all SQSs as seen from the standard deviation in table ..

		Spin up (eV)	Spin down (eV)	Total (eV)
$Cr_3Fe_3Mn_7Ni_3Si_{32}$	A	0.3390	0	0
	B	0.4745	0	0
	C	0.1342	0	0
	D	0.1950	0.0063	0.0063
	E	0.4211	0	0
$Cr_5Fe_5Mn_3Ni_3Si_{32}$	C	0.2103	0	0
	D	0.0674	0.0413	0.0372
	E	0.3619	0	0
$Cr_5Fe_3Mn_5Ni_3Si_{32}$	A	0.2082	0	0
	B	0.4053	0	0
	C	0.4659	0	0
	D	0.0843	0.0121	0.0121
	E	0.3008	0	0
$Cr_3Fe_5Mn_5Ni_3Si_{32}$	A	0.3922	0	0
	C	0.1285	0	0
	D	0.2595	0.1004	1.004
	E	0.3591	0.1003	0.0848

Table 8.6: Total and spin polarized band gap of 4 permutations of CFMN (fesi2) with PBE GGA calculation. The structures that are excluded from this list either failed in calculations, or does not show any band gap.

In this section we have seen that it's defintivly a merit for exploring the quasiternary phase diagram. We find the overall most stable composistion by increasing the number of manganese atoms in the composistion. Judging from the most stable supercells of the permutations, we can say that the high magnetic moment is attributed to chromium and manganese atoms as in the CFMN (fesi2) system. The same can be saif for the $Cr_5Fe_3Mn_5Ni_3Si_{32}$ alloy where we increase the proportions of the magnetic elements Cr and Mn relative to Fe and Ni. From these patterns observed in the permutations and the equal distribution of CFMN (fesi2), we can

conclude that the magnetic properties of this compound is reliant on chromium and manganese. This is also seen from the magnetism in the permutations where we reduce these elements, ie low magnetic moment. **Something on why one is more stable than the other, and why they all are more stable than equal dist.**

With reference to the band gap, we see from table .. that half-metalic is the most preferred state in most permutaions. This is in line with the eqvimolar distribution, as also here we observed severe spin polarization, mainly spin up, in addition to the semiconducting character. As was the case in CFMN (fesi2), we can not report any concise relation between the stability of the supercells and band gap, except for that the semiconducting SQSs is rarely the most stable of the set, but always above the mean total energy, the exception for this obviosuly being the chromium reduced alloy in which the two highest energy SQSs both were semiconductors. An interesting observation of the band gap is the relation to the magnetic moment. From table .. we see that the permutations differ in magnetic moment, but internly as highligted by the standard deviation we also note a variation in the magntic moment. And facinatingly, all reported semiconductors have the identical magnetic moment equal to 5.0000/48. The only exception is the eqvimolar system, were all structures had identical mag equal to 4.0000/48. Howver, this observation does not point to any domintating direction as this value is not the minimum or maxium magnetization, so we can not report a relation between high/low magnetization and the band gap.

As a conclusion to this segment we do not find one best direction to expore of the quasiternary phasediagram, as good and promising results was unveiled to some degree in all directions. This definitivly motivates the further exploration of the diagram, with the prospect of both improving the properties of the eqvimolar system and the ability to tune the properties by going in certain directions. In respect to the band gap, the most promising direction seems to be along manganese, as we see the most frequently large band gaps (in spin up) by increasing manganese, and the least frequent by reduction of manganese. For purely semiconducting compounds, reduction of chromium appears as a viable option seen from the 50% ratio of semiconducting to half-metalic ratio. An intersting proposistion for future work would thus be to reduce chromium and increase manganese simontainusly.

Conclusion example: In this project we have found many structures that show signs of semiconducting properties, but only CFMN fesi2 produced clear indication thorugh all 3 levels of meassures, ie eigenvalues, bandgap.py and dos, 3 levels of depth; PBE, SCAN, HSE06, and 5 levels of width, ie the 5 SQSs

Skriv i introducksjonen av resultater intensjonen vår med å nevne ting som stabilitet og magnetisme, og hvor overfladisk den analysen her. En ordentlig analyse av dette ville involvert mange flere jobber med ulike magnetiske konfigurasjoner og innstillinger. En stabilitetsavhandling ville invlovert grundigere relaksering og analyse av gitterparametere og celle, finite temperatur beregninger osv. Hovedvekten i

denne oppgaven er på båndgapet

Chapter 9

The bad (Other composistions)

In similar fashion to the preceeding section, we here list the mean and standard devitation of a set of SQSs for different high-entopy silicides of the fesi2 unit cell. The compositions we have selected in this segment is to a degree arbitratry aside from being 3d elements wi simply wish to observe the outcome of different alloys in respect to the band gap. The compositions are are eqvimolar distributions of $CrFeCoNiSi_2$ and CrFeTiNi where manganese is replaced by Cobalt, then Titanium. Furthermore $CrFeMnTiSi_2$ where the large Ni atoms are replaced by much smaller Ti, and $CoFeMnNiSi_2$ where Cobalt takes the place of Chromium. Keep in mind, that these SQSs were not simply created by replacing elements in the existing supercells of CFMN (fesi2), but rather generated through TDEP and the SQS theory to form 5 new distinct supercells per composistion out of the fesi2 unit cell, identical to how we tested CFMN (fesi2). Additontly, all supercells contain 48 total atoms as before.

	Toten (eV)		Enthalpy of formation	Mag	
CrFeCoNi	- 6.4655	0.0056	-12.7536	0.0083	0.0155
CoFeMnNi	- 6.4731	0.0046	-15.0836	0.0000	0.0000
CrFeTiNi	- 6.4217	0.0087	-7.5040	0.0305	0.0293
CrFeMnTi	-6.6994	0.0071	-7.3060	0.1142	0.0641

The first observation we make of table .. is that the total energy is much lower than CFMN, ie less stable **?**. The magnetization follows in line with the topics discussed above, clearly the magnetization is drastically reduced by removing either manganese or chromium. **Vent på svar fra O.M om å sammenligne energier/entalpi på tvers av sammensetninger**

Of the total 20 supercells we calculated in this compositonal spectrum, the overwelming majority are metals. In the CrFeCoNi composistion all SQSs were metalic, we perfomred additional calculations with the SCAN functional that corresponded well with the observed outcome from PBE. From the CrFeTiNi alloy we include the results of SQS A and B, where A display very small gaps in both spin channels with PBE of 0.039 eV and 0.002 eV, but no total band gap. This structure contain defect states in both channels, moreover the spin gaps are not observed in the density of

states. However this can could be becouse of low resolution in the density of states, as we observed in structure C in the CFMN (fesi2) SQS and some of the permutations. Our last meassure of calculating the bad gap from the pymatgen package point to a metal. From these conflicted results we can not with certainty confirm the observed band gaps in this SQS, as we did in CFMN were all methods were in agreement. We observe a smiliar case in B, the eigenvalues indicate a small total band gap of 0.008 eV and spin polarized gaps around 0.01 eV, in despite of defect states. But as in A, the gap is not found from other methods of evaluation or functionals.

In the two previous examples we replaced manganese with Co and Ti and found very limited sucsess in regards to our task of finding semiconducting high-entropy silicides. Replacing Cr with Co instead, yielded two semiconducting SQSs A and E. We note that these supercells lie around the mean total energy of the set, but the upmost stable SQSs are metals. The band gap in A is in good agreement throughout all 3 meassures to a value of 0.033 eV with PBE and 0.041 with SCAN. What's more the gap transision is consistent across both functionals in contrast to the results of CFMN (fesi2). Surprisingly, the band gap vanishes with HSE06 calculations (TBC). Using gaussian smearing with smearing width 0.005 and 20000 points to calculate the DOS yields a band gap of 0.039 eV. We have found previosly for CFMN (fesi2) that these calculations typically are in good agreement with TBC and reliable. On the other hand, the gap is not entierly visable in the density of states, and not found from bandgap.py, but this could be a consequence of the inaccuracy in DOS calculations both with gaussian smearing and a small number of k-points.

In E, we find a band gap of 0.0058 eV from both the eigenvalues and bandgap.py with PBE, and a lesser gap of 0.0037 eV with SCAN. The density of states is not zero at Ef as seen in figure**insert figure**, but show very small values that may indicate a band gap as we ahave experienced in other cases as well. On the grounds that we find complemetary band gaps with both SCAN and PBE from eigenvalues and bandgap.py and no defect states in the eigenvalues, we conclude that this band gap is legitimate despite of the DOS values. We relate this result to the low resolution of 2500 points in calculating the density of states, considering that the gap is very narrow. **Wait for HSE06**

In the final composistion of fesi2 based high-entropy silicides tested in this project, we replace Ni atoms with much smaller Ti. As stated in the introduction we find the highest magnetic moment of all composistions with this arrangement, due to the inclusion of both chromum and manganese in the structure. **Most stable?** Among the 5 SQSs of this particlar mix, there is a significant variation in the magnetic moment between supercells, the lowest observed magnetic moment is 0.04 in E, and the highest 0.20 in B. We recognize a clear distinction between stability and magnetisim in this compound, the 3 lesser magnetic SQSs have very comperable hig total energy, and the two highly magnetic supercells are notebly less stable.

Write in the conclusion somewhere: In this project, we have read the band gap from our own written script where we evaluate the eigenvalues

from the EIGENVAL file in vasp, used a script called bandgap.py from pymatgen, and considered the density of states. In the structures where we report a band gap, all these 3 have corresponded, additiontly the SCAN functional all though most frequently alter the value, agree on the presence of a band gap. However, we have found other structures where the eigenvalues show a small band gap. But due to the fact that the eigenvalues contain defect states, and nonphysical occupancy, the valididty of these resuslts are uncertain, and we do not include them unless they are observable from the other methods mentioned above. We will however include some of these in the discussion.

Chapter 10

The ugly (Other symmetry groups)

In the discission above we have covered in great detail the possibilites of high-entropy silicides based on the $\beta-$ FeSi$_2$ unit cell with twice as many silicon atoms to 3d elements. The primary outcome and conclsion of this research was that particularly the combination of Cr, Fe, Mn and Ni resulted in superiour properties in the light of the motivatian behind this project. The next question we wish to answer is if ihe promising results of the CFMN system be reproduced in other symetries. In this section we will implement the CFMN composistion in crystal structures based on hexagonal CrSi$_2$ ($P6_{422}$), both tetragonal and orthorombic Mn$_{16}$Si$_{28}$ ($P\bar{4}c2 and$, $Pcca$), and trigonal Fe$_2$Si ($P\bar{3}m1$) where we test the CFMN system to varying metal and silicon ratioes, and crystal structures. As before, the total energy, enthalpy of formation and magnetic moment per atom can be found bellow in table ..

	Total energy per energy		Enthalpy of formation	Mag per atom	
CrSi2	-6.4837	0.0087	-8.1205	0.0887	0.0387
MnSi	-6.6658	0.0071	-9.1848	0.0687	0.0398
Fe2Si	-7.5082	0.0107	-10.2474	0.3848	0.0588

CrSi2 From our calculations with PBE DFT we find the bulk crsi2 material to be an indirect semiconductor with a band gap of 0.33 eV, slightly bellow the listed value of 0.36 eV in materials project **cite**, suprinsingly we find a smaller gap of 0.32 eV from the SCAN functional. The compound is also nonmagnetic in agreement with materials project. Fore the bulk material we employed a 9 atom cell, with 6 silicon and 3 cr atoms, from this we generated SQSs of 72 atoms with the same ratio. **Include toten per atom for the unit cell? and figure of SQS + unit cell?**. For this given composistion and system we observe very similar results to that of the compositstions discussed above, the eigenvalues of several SQSs report a small band gap, but its not apperant from neither the density of states or from the bandgap.py script of pymatgen. Additiontly, we can not repreoduce the gap with the SCAN functional, as was possible for the

CFMN (fesi2) system.

MnSi In the tetragonal configuration, the bulk material is a nonmagnetic indirect semiconductor with a band gap of 0.76 eV acoording to our PBE calculations, and 0.78 eV from SCAN. Materials project find a band gap of 0.76 eV, in good agreement with our own PBE results. The unit cell consist of 44 total atoms, 16 manganese and 28 silicon. In the orthoromibic cell, with equal number of elements we find a band gap of 0.76 eV (0.77 ev SCAN) as well. In contrast, the CFMN alloy of both these cells produce metalic compounds. It should be noted that structures B and D in the tetragonal ssystem did not fully relax, same for D in the orthorombic cell, so these results could be inaccurate.

Fe2Si In this cell, we drasticly alter the metal-silicon ratio, this is seen both in the band gap and magnetic properties of the material. The magnetic moment of this cell consisting of 4 iron atoms and 2 silicon atoms is 0.67, from the iron atoms. This magnetic charachter can also be observed from the discrepency between the two spin channels. In spin down we find a band gap of 0.21 eV, while there is no gap in spin up. This gap can also be seen in the density of states **Include figure**. This however is an abnormal result in regard to other experimental work and littereature on the Fe2Si **cite** $https$: $//www.sciencedirect.com/science/article/pii/S0925838816329796?casa_token =$ $g9DRpU9IClcAAAAA : 6Gd12A4Kh9J2igUWMVwHN8OSIKzD27VACA052FNsSAWhRY6PE$ Our results are subject to errors, particularly we note that the eigenvalues used to calculate the gap contain nonphysical values in the spin down channel. However, the gap is evident in the density of states thus we include the result in this report, but acknowlendge the uncertainties revolving the value.

From this unit cell we generate 54 atom SQSs. From table .. we see that the magnetic nature remains, producing the overall highest magnetic moment of all studied supercells, which is not a surprising result considering the 3d metal to silicon ratio. **More on magnetic and total energy.** The magnetism can also be seen in the difference between the two spin channels, the bands where the occupancy transistion from 1 to 0, ie occupied to not occupied is very different. In the most magnetic supercell D, we saw a distance of 22 bands between the spin down transistion and spin down transistion. Most supercells are metals from our PBE calculations. B and D show a very small gap of around 0.01 eV in one spin channel. In E we find a very narrow gap semiconductor with a total gap of 0.002 eV. This gap is surrounded by the same uncertainties as discussed previosly.

Chapter 11

The overview

Summary and discussion of all results.
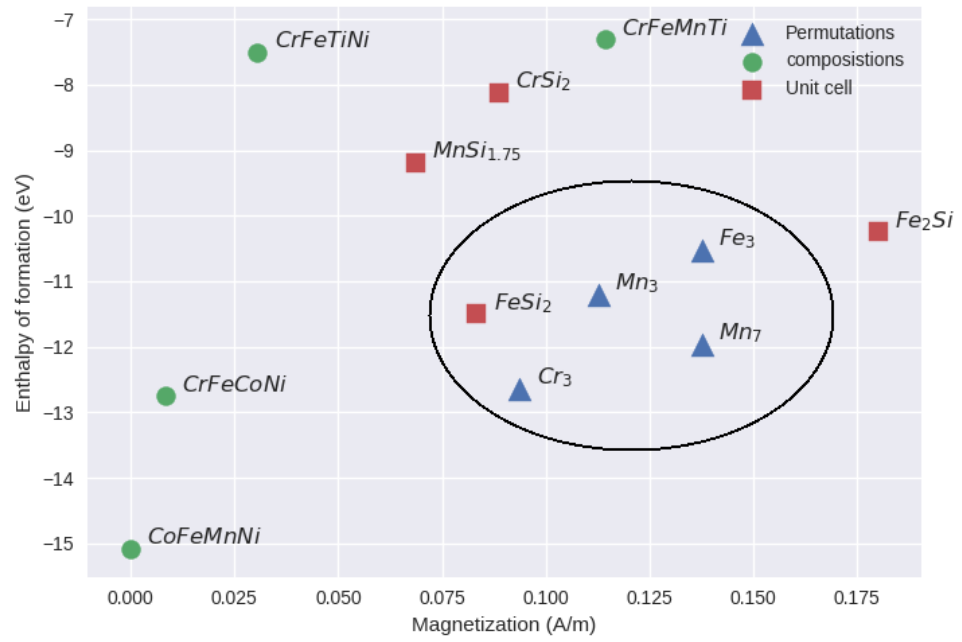
Part IV

Conclusion

Write conclusion here